Flight Nutation Validation of the COS-B and EQUATOR-S spacecraft

J.M. Kuiper[1]
Chair Space Systems Engineering – Faculty of Aerospace Engineering
Delft University of Technology, The Netherlands
j.m.kuiper@tudelft.nl

Summary

The validation of spacecraft flight nutation damping performance can only be obtained when flight data become available. Dedicated space nutation tests, e.g. in a decommissioning phase, are required to enable a systematic evaluation of model, ground test and space performance results. Space nutation flight data, however, are sparsely available. This article deals with the verification and validation of the COS-B and EQUATOR-S nutation flight data on basis of ground test and three types of models. It will be shown that the Navier-Stokes model solution used in the development of the Ulysses and FY-2 nutation dampers is the backbone of liquid damper design of the type "tube-with-endpots".

1 Introduction

The flight nutation performance data of a series of spinning spacecraft (S/C) given in Table-1 was studied. The S/C were selected for reasons of availability of their Nutation Damper (ND) design heritage, flight and ground test as well as qualification data. The given spacecraft refer to different mission classes: Meteorological (3, 4) in GEO orbit and purely scientific [1, 2, 5, 6]. From the latter class #2, 5 and 6 are in highly elliptical Earth orbits whilst #1 is in a solar elliptical orbit. The Attitude and Orbit Control System (AOCS) of S/C #5 and #6 incorporates a pair of meridian type NDs, shown in Fig-3, which are mounted at radius R_m perpendicular to the equatorial Centre-Of-Mass (COM) plane. All other S/C are equipped with a pair of equatorially mounted NDs which are mounted at a height $Z = Z_0$ above the COM equatorial plane at $Z = 0$.

The only traceable useful space test validation data are from the COS-B S/C [Bongers, 1984] and the EQUATOR-S S/C [Häusler at al., 2002] mission. The applied nutation dampers (NDs) are both of the meridian type with comparable design driving requirements as becomes clear from Table-2 in Chapter 4. A cross verification of models using experimental results on ground and space flight data is therefore the key to analyze the differences systematically.

Table-1 *Selection of nutation damping V&V missions.*

V&V candidate	S/C	Prime contractor and/or Principal Investigator	ND type[1]	Spin-rate [rpm]	Lifetime
1	Ulysses	ESA/NASA	E	5	1990-2008
2	Cluster	ESA/NASA	E	5	2001-
3	FY-2	Chinese GWIC	E	100	1994-
4	MSG	ESA/Eumetsat	E	100	2002-
5	EQUATOR-S	Max Planck	M	48	1997
6	COS-B	ESA	M	10	1975-1982

[1] E=equatorial, M= Meridian

In the exploration of the applicable nutation damping theory different models were distinguished and compared. This article is dedicated to the verification and validation (V&V) of these models whilst the modeling itself is released in [Ancher, 1977], [Bakel, 1993], [Batchelor, 1980], [Häusler, 2001 and 2002], [Hughes, 1966], [Loitsyanskii, 1966], [Muto and Nakane, 1980], [Truckenbrodt, 1996] and [Womersley, 1955].

The first step is the verification of the model predictions by scaled ground tests using a Performance Test Model (PTM). This typically happens during the phase B of a Nutation Damper (ND) project and is essential to convince the customer (prime contractor) of the health of the design. After the Preliminary Design Review (PDR) milestone is successful the go ahead is given for the extended test and production phase C/D of the qualification (QM) and the flight models (FM).

The ultimate ground test system, to verify and validate flight ND damping performance, is either a horizontal pendulum arrangement like the air bearing test setup at Dutch Space [FDS, 1992] or a vertical pendulum [Häusler and Eidel, 2001]. The ground test equipment will be discussed as primary instrument for verification of the ND model predictions.

[1]Scientific staff member - Chair Space Systems Engineering – Faculty of Aerospace Engineering

2 Verification and Validation data

2.1 METEOSAT

The meteorological European Meteosat Second Generation (MSG) and Chinese FY-2 S/C in Table-1 are both member of the class of 100 rpm geostationary spin-stabilized spacecraft. The nutation of the sophisticated MSG S/C is dealt with since limited V&V flight data was only traceable only for tis S/C. The MSG NDs are of the equatorial tube-with-endpots type and made by URENCO, The Netherlands. The author was involved independently in the pre-phase A study questions from Marconi Space Systems as subcontractor of Aerospatiale Cannes [Crowden, 1990], i.e., to supply a basic ND design and a Rough Order of Magnitude (ROM) costs estimate. The MSG flight validation data is given by [Weymiens et al., 1999], [Luengo, 2004] and [Ebert and Reger, 1994].

The MSG S/C incorporates the imaging instrument SEVIRI (Spinning Enhanced Visible and Infra-Red Imager) which is capable to provide measurements of stars, Earth horizon and landmarks, apart from meteorological images. The author was involved as a system engineer in the design team of the SEVIRI passive radiant cooler as well [Boyd and Kuiper, 1996].

The following types of MSG nutation damping are considered:

Nutation damping and tank sloshing
The nuational damping may reveal sharp resonance effects at particular propellant tank fillings. This effect was studied for MSG by [Ebert and Reger, 1997]. The authors state that liquid inertial modes and S/C nutation are strongly resonance related and may explain the strong variations in in-orbit tests on INTELSAT V and in airbearing tests given by [Agrawal, 1993].

Nutation due to scan mirror movements
The MSG nutation due to the Spinning Enhanced Visible and Infra-Red Imager (SEVIRI) scan mirror movements is dealt with by [Luengo, 2004]. The SEVIRI instrument contains a 20 kg mirror that rotates around an axis parallel to the S/C X-axis with the Z-axis being the S/C spin-axis. The equatorial NDs are mounted on the Y-axis. The SEVIRI mirror rotation can be described as an initial stage in which the mirror is repositioned (retraced) in the starting point to obtain the meteorologocal data, a second Black-Body calibration stage at fixed position and a final scanning stage to acquire the image. The mirror movement induces a variation in the S/C inertia matrix and as a consequence modified rotations thus S/C nutation during the scanning and retracing phases. A dynamical model, including the NDs, is given by [Luengo, 2004] and uses a simple model with only viscous damping. The worst case performance yields a time constant τ = 2 min compliant with the requirement $\tau < 4$ min [Weymiens et al., 1999]. The maximum impact in between two nominal cycles equals $\Delta\omega_y = 0.5$ [mrad/s] angular velocity about the principal inertia Y-axis. The results comply with the ND performance design data and comply very well with the results extracted from telemetry data. This is, beside a confirmation of the correctness of the applied models, a proof of the ND nominal performance. The strong ND performance model proofs, however, will be extracted from the EQUATOR-S and especially COS-B flight data in the following Chapters. First the two missions are briefly regarded, secondly the terrestrial test equipment for the scaled ND performance experiments is described and finally the validation by flight data will be considered.

2.2 EQUATOR-S

The EQUATOR-S S/C mission was designed and developed at the Max-Planck Institute in Garching with some supplementary items from agencies and industry. The S/C was launched the 2nd of December 1997 into an elliptical Earth orbit (perigee 479 km, apogee 67,275 km, inclination 3.9^0 and T=22.3 hour). The science mission included magneto-spherical plasma and field measurements in the frame of ISTP (International Solar Terrestrial Physics Program).

The meridian EQUATOR-S NDs are shown in the right picture of Fig-1. Its build standard is derived from the AMPTE-IRM S/C meridian ND [Truckenbrodt et al., 1982] and shown in Fig-2. The endpots are adhesive fastened whilst the Fokker tube-with-endpots NDs are electron beam welded. Space validation data for the EQUATOR-S operational case are given by [Häusler and Eidel, 2001] and [Häusler et al., 2002].

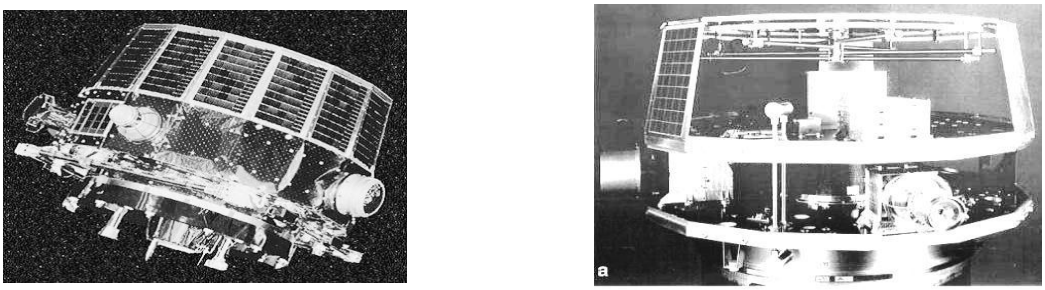

Fig-1 *EQUATOR-S S/C (left picture) [Haerendel et al., 1999] and (right picture) the interior of the S/C showing one of the two meridian NDs vertically mounted [Häusler et al., 2002].*

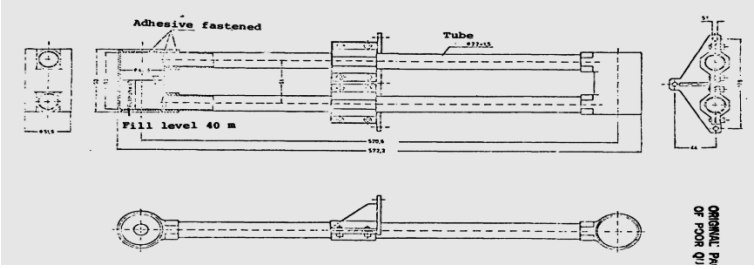

Fig-2 *AMPTE ND build standard [Truckenbrodt et al., 1982].*

2.3 COS-B

The COS-B scientific mission [Willmore, 1970] was to study in detail the sources of extra-terrestrial gamma radiation at energies above about 30 MeV. The successful COS-B space missions had no optical telescopes or complicated scientific instrumentation. Its only function was to point in the direction of a star or other object and measuring its gamma-ray emissions. COS-B was an ESA mission, built and equipped by European scientists and launched by NASA. It was ESA's first satellite dedicated to a single experiment enabling an extensive survey of the galaxy in the energy range 50 MeV to 5 GeV. The spacecraft overall mass equals 278 kg and the attitude measurement accuracy 1^0. Its cylindrical sizes are a height 1.2 m and a diameter 1.4 m. The 37-hour orbit of COS-B was an eccentric orbit (launch 1975-08-09, perigee 350 km, apogee 100,000 km, inclination 90^0) that ensured that the satellite was outside the Earth's radiation belts for most of the time [COS-B, 1975]. The end of the mission coincided with the end of its propellant supply, which had been conserved by careful choice of maneuvers. The originally foreseen duration of the mission was two years, but COS-B was finally switched off on 25th April 1982, having functioned successfully for more than 6.5 years. In spring 1982 a dedicated series of space nutation experiments were executed at different frequencies and initial nutation angles induced by thruster firing. The rich amount of COS-B nutation modeling, ground verification and space operational validation data is given by [Bongers, 1984]. The position of the NDs in the spacecraft is shown in Fig-3.

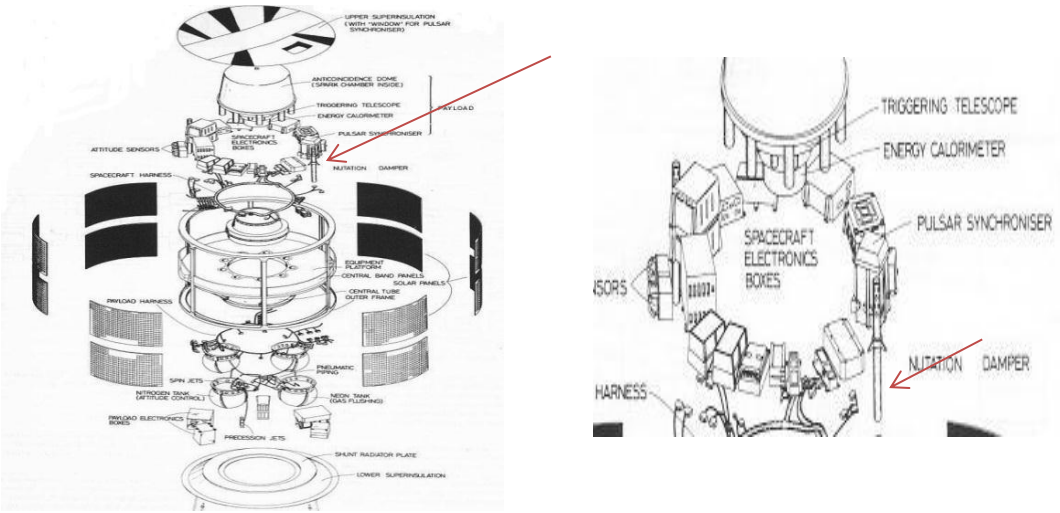

Fig-3 *COS-B S/C exploded view (left) and the upper stage zoomed-in to show the meridian NDs* [COS-B, 1975].

3 Airbearing Pendulum Tests

3.1 Vertical Pendulum

The vertical plane pendulum used [Häusler et al., 2002] to verify the EQUATOR-S meridian ND performance is shown in Fig-4. In the left picture the two black contra weights are visible along the vertical rod whilst the (faintly visible) plexi-glass scale model is at the lower side. This scale model is enlarged in the right picture. In this pendulum configuration with horizontal axis, springs are not required. The angular dependent gravitational acceleration is taken into account in the Euler-Lagrange equations of the damper liquid motion.

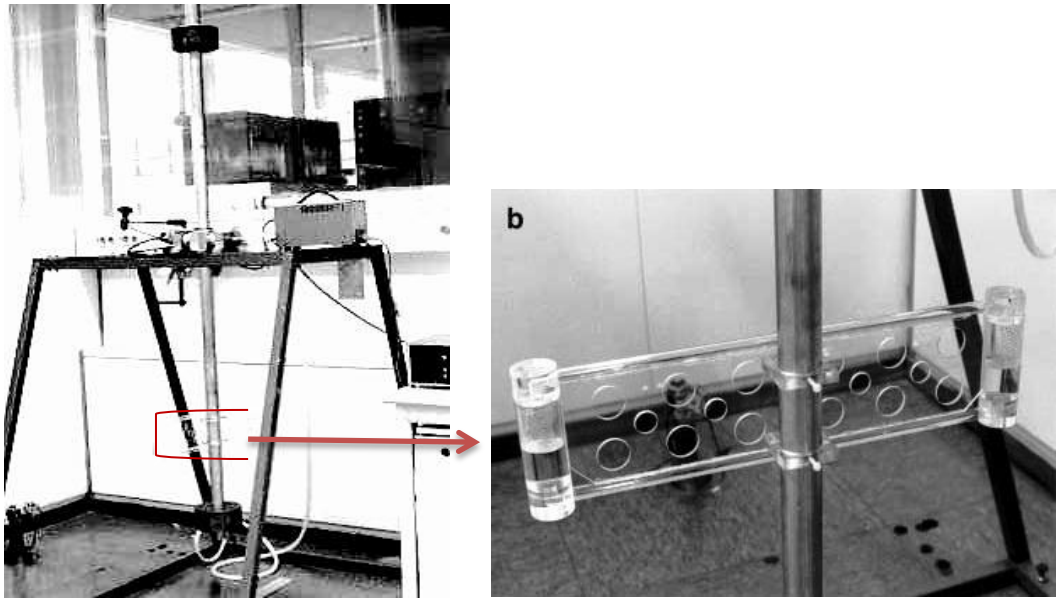

Fig-4 *The vertical pendulum for ND performance verification used by* [Häusler and Eidel, 2001].

3.2 Horizontal Pendulum

The setup of the Fokker ND performance measurement setup with tests oscillations in the horizontal iso-gravity plane is shown in Fig-5. The zoomed-in picture at the right side of Fig-5 shows the central air-bearing hub, the oscillation springs and the ND attachment rail at the end of the mounting arm. One of the two wire-suspended arms is recognized as well as the two oscillation springs which provide the harmonic driving torque. For stiffness and stability reasons a steal test-arm with square intersection and length R_a = 2 m was chosen. This limits torsion and linear arm oscillations down to < 1% disturbing accelerations of the ND liquid damping performance to be tested. The digital angle read-out - an optical encoder - and computer system are integrated to monitor the oscillation angle with 2.75" resolution.

The spacecraft nutation is simulated by the oscillatory movement about the vertical rotation axis. The desired pendulum time is provided by two adjustable springs and/or additional masses. The horizontal pendulum with vertical axis uses the gravitational 1-g force to scale ("replace") the flight centrifugal acceleration. Visible in Fig-5 are the suspension wires of the ND arms and the oscillation springs. The NDs themselves are not attached.

The damping performance at very small angles is analyzed after automatic recording and processing of the normalized damping versus the angular amplitude. The latter is given by $R{\cdot}\Phi(t)$ over the specified amplitude range with R the mounting arm length and $\Phi(t)$ the momentary air-bearing oscillation angle.

The damping performance verification is initially obtained by Performance Test Model (PTM) scale tests. In a later project phase this is done in addition by the Qualification Model (QM) and Flight Model (FM) air-bearing performance tests.

The air-bearing arm length R and its Mass-Of-Inertia (MOI) I_0 are independent of scaling rules. On basis of measurement accuracy trade-offs a compliant arm length is chosen. The radius for the FY-2 ND was e.g. taken R = 2000±5 mm with total MOI 199.1 kg·m^2 using two dummy models (DMs) without damping liquid or 190–200 kg·m^2 with two PTMs. The difference is attributed to the 'free' sloshing motion of the damping liquid in the endpots of the ND. For other ND projects specific choices and trade-offs are made on the arm lengths and the required stability as imposed by the ND test plan.

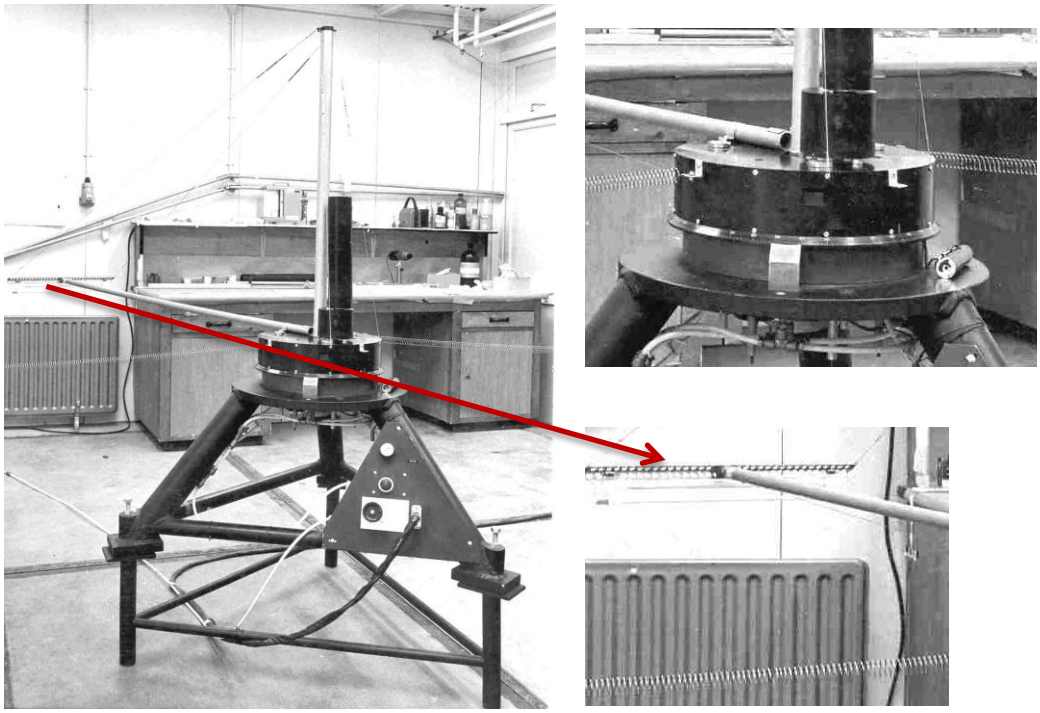

Fig-5 *The air-bearing setup for the ND damping performance tests at Dutch Space in 1990. The red arrow indicates the support rail for the ND which is not attached.*

The exponential damping time constant τ_i is found using single logarithmic plots of the amplitude $R\Phi(t)$ recorded over a time range $\Delta t = t_e - t_0$ using 4 to 5 logarithmic units, i.e., $\ln[\Phi(t_0)/\Phi(t_e)] = 4$ to 5 with

$$R_a\Phi(t) = R_a\Phi_0 e^{-t/\tau_i}. \tag{1}$$

The time test range is related to the required nutation angle range prescribed by the specific ND project requirements. The ranges are scaled according space-to-ground fluid mechanics scaling rules.

By shifting the extra weights on the test arms the oscillation frequency can be varied. The net ND damping time constant τ_{ND} is finally obtained by

$$\frac{1}{\tau_{ND}} = \frac{1}{\tau_1} - \frac{1}{\tau_2} \tag{2}$$

with τ_1 the test damping time constant using a PTM, QM or FM and τ_2 the test damping time constant using a dummy model (DM). The time constant τ_2 refers to the same test but with the PTM, QM and FMs replaced by dummy models. These DMs have the same mass and geometry; contain no liquid but additional mass to compensate for this. This enables the separation of the liquid damping performance from the friction of the air-bearing and air resistance. The reduced time constant τ_{ND} approximates the time constant of the nutation liquid damping only. The influence of the test room air-environmental damping and air-bearing friction are therefore eliminated in best terms by applying Eqn. (2). The exponential time constant related to the normalized damping rate $P(t)/a_o^2$ as test parameter with $P(t)$ the time dependent dissipation and a_o^2 the squared nutation or test acceleration is given by

$$\frac{1}{\tau_{test}} = \frac{R_a^2\Omega^2}{I_{tot}}\left(\frac{P}{a_0^2}\right)_{test} \tag{3}$$

with $I_{tot} = I_0 + 2I_{ND}$ the total inertia about the vertical air-bearing axis, I_0 the test arm MOI including resonance tuning weights and I_{ND} the additional inertia due to the test ND thus the PTM, DM, QM or FM.

Eqn. (3) enables the determination of the time dependent $P(t)/a_o^2$ value which gets constant only in the laminar oscillation range at very small angles. The exponential damping time constant τ_{test} depends on the air-bearing radius, its MOI, the airbearing angular test frequency and the damping rate of the test model (PTM, QM, FM and DM). Finally by scaling the 1-g damping rate towards its space value, the performance of the FM as function of the S/C inertia ratio λ is found. As basic rule five λ values are taken as minimum number to define a proper performance check of the FM design. A number of precautions is taken to obtain optimal test conditions and accurate results:

- The total MOI of the air bearing including the test-setup and the NDs (or DMs) is measured
- The oscillation arms generate airflows. This effect is reduced by doing the same measurements with DMs and applying Eqn. (2). Additional disturbance effects, possibly caused by people walking around or accidental (random) ventilation flows, are avoided. It was proposed by the author to do tests with aerodynamic (ellipsoidal encapsulation) profiles attached to the end of the arms around the attached NDs to limit and control the additional airflows even further
- NDs are leveled using a theodolite within ±10 arcsec
- The air-bearing feet are adjusted up to the level where the end of the arms are within 20 arcsec variation over the full 360^0 of angular range at 5 PSI air-bearing operational pressure
- The moving damper liquid exerts a torsional moment on the mounting arms. To limit vibrations the torsional material stiffness G [Nm/rad] of the test arms is chosen to limit torsional accelerations down to 1% of the maximum tangential value. The G value is verified by applying a zero and a well-defined torsional moment on one end of the mounting arm whilst theodolite measurements are made with a mirror at the end of the arm
- The same kind of engineering arguments hold for the trade-off on the effective test arm length which is driven by a < 1% relative magnitude of the centrifugal to nutation acceleration
- The centrifugal flight acceleration field is curved whilst the terrestrial 1-g field is straight. This implies a curved FM and a straight PTM. However in general the FM NDs are chosen straight as well as the PTMs. The effect on the damping performance is negligible. To prove this, consider a straight ND in a curved acceleration gravity field. It is clear that the acceleration decreases in the left part of the liquid tube is compensated by an equal increase in the right part. The same argument holds for a curved ND in a straight 1-g terrestrial gravity field.

4 EQUATOR-S and COS-B Data Analysis

The main spacecraft and ND design data are given in Table-2. In the last rows the relative ND liquid mass and the factor k_0 is given. The factor k_0 accounts in the refined Hagen-Poiseuille model [Häusler et al., 2002] for the effective relative amount of damping liquid mass.

The amount of COS-B liquid mass m compared to the S/C mass M, with requirement $m/M << 1$ as prerequisite of a quasi-rigid S/C configuration, is about one third of the EQUATOR-S value whilst the k_0 factor is comparable. The 5" extreme nutation angle for COS-B and the less than 0.5" per orbit drift requirement follow from the X-ray science experiment requirements [Willmore, 1970].

Table-2 *COS-B [Bongers, 1984] and EQUATOR-S [Häusler et al., 2002] meridian ND design data.*

S/C	**COS-B**	**EQUATOR-S**
S/C total mass M [kg]	278	216.9 (dry mass)
[source]	[ESA, 2001]	[Enderle et al., 1997]
Spin axis inertia I_{ZZ} [kg.m^2]	54.53	34.35[a] to 38[b]
Spinrate (nom) [rpm]	10 ± 0.1	48[a] to 50[b]
BOL inertia ratio λ_0 [-]	1.232	1.330
Nutation amplitude [degree]		
• Initial	3.8	3.3
• Final	< 5"	< 1.0[c]
Temperature [deg C]	-20 to +30	+12.7 (nomimal)
Hardware model	FM PTM	FM PTM[d]
Materials liquid / housing	PP1/ Al PP1/ Al	PP1/Al H_2O/Plexiglass
ND time constant [sec]		
• Theory (NS, RHP)	see multiple cases in text	38.7 (RHP) 72.3 (RHP)
• FM space / PTM ground test		38 ± 3 (RHP) 72 ± 6
S/C mounting radius [mm]	668	565
Design dimensions <a, b, L, H> mm]	4.0, 20.96, 400, 40	5.0, 23.04, 500, 80
FM/PTM damping liquid	PP1	PP3
FM /PTM ND liquid temperature [^{0}C]	9.9 18-21	12.7 18-21
ND liquid mass m [kg]	0.136	0.291
ND liquid mass ratio m/M [%]	0.049	0.134
RHP k_0 factor [-]	0.473	0.374

[a]Booms folded [b]Booms deployed [c]Range taken from Fig-6 [d]Not flight representative

4.1 Applicable Models

Four applicable models are dealt in the given sources in the introduction. In the frame of the nutation Verification and Validation (V&V) analysis they are briefly summarized:

- The **first** Hagen-Poiseuille (HP) model considers a fully developed single directional flow which is in general not valid due to the harmonic nutation sweep-up forces in the liquid tube. Only at low S/C spin-rates with consequently low nutation frequencies the model can be used. The HP model is a special class of the generic Navier-Stokes solution. The HP model proved to be well applicable to describe and quantify the natural resonance behavior at sweep-up moments of nutation in performance verification tests.
- The **second** Refined HP (RHP) model [Häusler et al., 2002] is an adapted version of the HP model based on the theory derived by [Truckenbrod, 1986].
- The **third** NS model was derived by solving the Navier Stokes Equation (NSE).
- A **fourth** ND model [Crellin, 1982] applied at ESTEC/ESA is also based on the solution of the NSE. The model was used beside the Fokker Space NS model in the Ulysses anomaly study in the period November/December 1990. The results agreed seamless though different inertial systems are used.

The Hagen-Poiseuille (HP), its refined EQUATOR-S version (RHP) and the Navier-Stokes (NS) models with common NS basis were all used to analyze the differences in flight and ground test results. In the following sections the model differences will be explained.

4.2 EQUATOR-S S/C Nutation

The EQUATOR-S ND design was driven by the RHP model from [Häusler and Eidel, 2001] based on [Truckenbrodt, 1968]. It enabled a compliance in the modeling results, air-bearing test results and flight nutation data of the 48 rpm spin-stabilized EQUATOR-S S/C. The RHP model derivation starts from the generic case of communicating vessels with, in addition, an inertia correction factor to account for the moving liquid mass in the dampers. The determination of the flight operational damping time constant is shown in Fig-6 with the detected nutation angle versus the elapsed flight time. The RHP time constant model results are in good agreement with EQUATOR-S ground test and in orbit nutation data [Häusler and Eidel, 2002]. The application of the RHP model however, revealed substantial differences compared with the NS model results. These will be further analyzed to study the validation range of the diverse models.

In Fig-7 the results of RHP, NS and HP modeling are shown. First the EQUATOR-S results from [Häusler and Eidel, 2001] and [Häusler et al., 2002] were verified (model calibration) by embedding their RHP model in MathCad® code beside the NS as well . The tuning parameter is the nominal inertia ratio $\lambda_0 = I_Z/I_x$ with I_Z the inertia about the spin-axis and $I_x = I_y$ the inertia about the perpendicular lateral axis. Taking their nominal inertia λ_o = 1.33 maximum damping design case at the nutation frequency Ω_o = 1.661 rad/s with endpot diameter 2b = 46.08 mm and liquid tube diameter 2a = 10 mm as calibration case, yields seamless model agreement. The MathCad® models deliver an exponential damping time constant τ = 50.330 s (NS) and 50.332 s (RHP) versus RHP value 50.33 s from [Häusler and Eidel, 2002].

Flight validation

The final flight design (2b = 45 mm, 2a = 9 mm) value differs slightly with τ = 69.3 s (RHP) versus 72.3 s from the [Häusler et al., 2002] RHP model. The flight validation value equals τ_{exp} = 72 ± 6 s as derived from Fig-6. The NS model value can be read from Fig-7 at the nominal nutation frequency Ω_o = 1.661 rad/s compliant with λ_o = 1.33 and equals τ = 61.3 s.

In Fig-7 the time constant differences between the NS, HP and RHP model predictions at λ_o = 1.33 are within 15% whilst the flight value is within the range of the NS and HP model.

In the horizontal direction the optimal inertia ratios, i.e. with minimum damping time constant, all show significant off-sets compared to the desired nominal inertia λ_o = 1.33 which means a mistuned ND resonance condition. The RHP model shows a -3% off-set whilst the NS and HP model show a -5% offset. It is remarkable that the EQUATOR-S ND design data [Häusler and Eidel, 2001] and [Häusler et al., 2002] do not reveal an essential picture like Fig-7 with the RHP model damping time constant as a function of either the nutation frequency Ω or the spacecraft inertia λ.

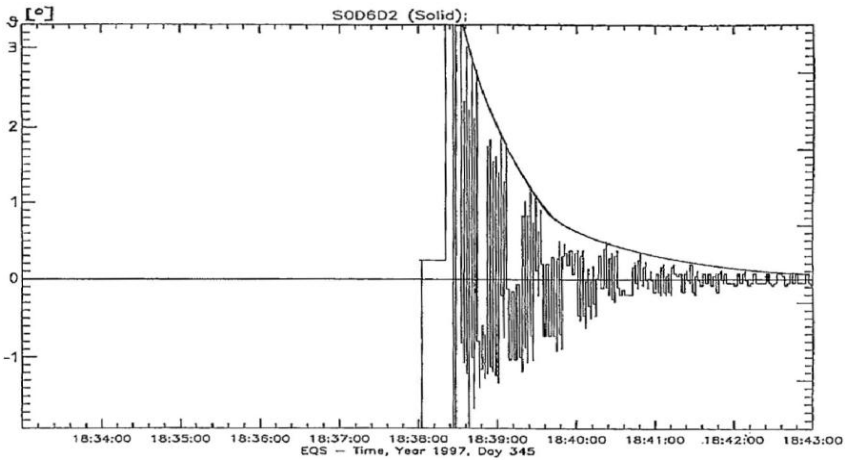

Fig-6 *Nutation angle attenuation of the EQUATOR-S S/C measured in flight which yields the flight validation value* τ_{exp} *= 72 ± 6 s [Häusler and Eidel, 2002].*

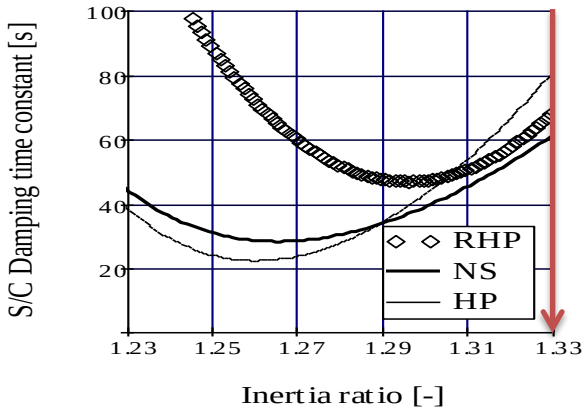

Fig-7 *EQUATOR-S S/C flight nutation time constant prediction at T = 12.7* ^{0}*C by three ND models with the arrow indicating the desired tuning condition.*

Ultimate nutation angle

The EQUATOR-S flight data show a minimum nutation angle < 0.1 deg. No additional test data or test philosophy is given to investigate the ultimate damping angle as was done for the COS-B S/C to follow.

4.3 COS-B S/C Nutation

The EOL COS-B S/C flight nutation data were analyzed by [Bongers, 1984]. The COS-B AOCS was equipped with two meridian NDs, shown in Figs-3 and 8. In the upper picture of Fig-8 the liquid and vapor tube, as well as the endpots are partly disguised by its structural housing. The lower picture shows the A-A cross-section with the liquid tube (a = 4 mm) at the bottom.

Nutation experiments were executed during spring 1982 at the S/C End-Of-Life (EOL) cycle. The nutation was induced by thruster firings up to angles of 3.8 degree. The nutation behavior was extracted from the sun sensor telemetry data and analyzed by Fast Fourier Transform (FFT) analysis from the S/C oscillatory behavior, a method described by [Wertz, 2003]. The ND flight performance complies well with the NS model predictions. The basic uncertainty in the modeling results is caused by inaccuracies in the Moments-Of-Inertia (MOI) values with < 2% absolute error, temperature and position angle of the NDs.

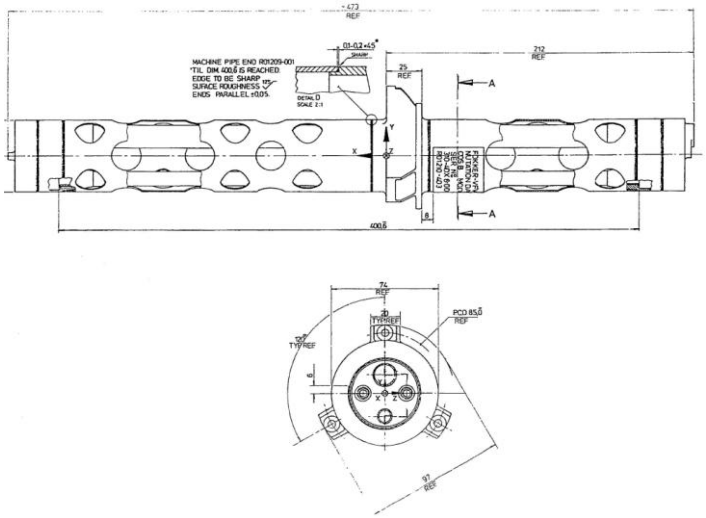

Fig-8 *Meridian COSB nutation damper built by (Fokker) Dutch Space [FDS, 1992].*

Taking these into account the re-analyzed and NS model verified results from [Bongers, 1984] are:

1. The nutation decays exponentially in all cases.
2. No correlation exists between the initial nutation angle and the time constant.
3. The in-orbit time constants, resulting from invoked flight nutation at 9.45 and 17.63 rpm, comply well with the results obtained by NS modeling and air-bearing tests.
4. Air-bearing PTM results comply well at lower spin rates (8 rpm)
5. At the high spin-rates 36.6 and 113.4 rpm the air-bearing tests predict less damping and consequently higher time constants.

The Fokker Space models as well as their test setup were improved since the development of the COS-B ND according to [Bongers, 1984] up to the standard used in the design and qualification of the Ulysses and FY2 nutation dampers.

Flight validation

The end-of-life (EOL) space nutation experiments [Bongers, 1984] were re-analyzed at the low spin-rate range ω_z = 9.45 ± 0.06 rpm and at the higher range ω_z = 17.63 ± 0.02 rpm with inclusion of the RHP model beside the NS and HP model. In Fig-9 the HP, RHP and NS model results are shown at 9.45 rpm spin-rate with all other parameters nominal as defined by Table-2 and a ND position angle $\alpha = 40^0$ in the equatorial plane with respect to the X-axis.

The NS and HP model results show a resonance shift of +5% beyond the specified EOL $\lambda_o = 1.232$ value whilst the RHP model shows a shift of 9%. Moreover the shape (less bandwidth) of the RHP curve differs. The NS and HP curve almost coincide as expected at low spin-rates.

The result at the EOL value $\lambda_o = 1.232$ agrees seamless with the space experiment results, i.e. the flight damping time constant τ = 7.0 min with standard deviation σ = 0.5. The same shifts hold for the model predictions of the nutation performance at 17.63 rpm spin-rate given in Fig-10. The result at $\lambda_o = 1.232$ matches again seamless with the results given by [Bongers, 1984] since the extracted flight damping time constant τ = 4.2 min with standard deviation σ = 0.3. In both cases the RHP model and its time constant prediction is far off and does not apply to the COS-B design and its flight performance validation.

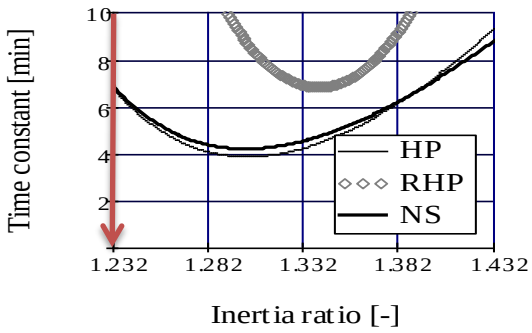

Fig-9 *COS-B nutation damping prediction by the HP, RHP and NS models at 9.45 rpm. The arrow indicates the desired tuning condition.*

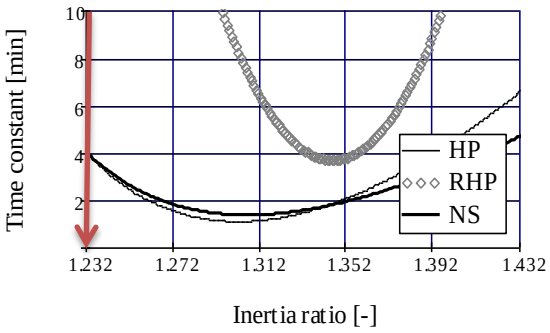

Fig-10 *COS-B FM damping prediction by the HP, RHP and NS models at 17.63 rpm spin-rate with the arrow indicating the desired tuning condition.*

Ultimate nutation angle

The contact angle hysteresis below the required 5" flight nutation angle is not experimentally detectable. Therefore a scaled experiment was executed [Dutch Space heritage] with a glass-water PTM model. The experiments were executed down to air-bearing angular motion levels representative for flight nutation angles < 0.2". Because of the low accuracy, caused by air-bearing turbulence flow phenomena in this range, a large number of repetitive experiments were necessary. The experimental values are valid in the vicinity of the flight spin-rate ω_z = 0.661 rad/s equal to 0.105 Hz in Fig-11. The results were re-analyzed and the verified results are given in Fig-11 with conclusions:

- The measured (marked) normalized damping values P/a_o^2 are determined at 1" and 0.2" equivalent flight nutation angle and do not show a significant difference in damping performance. At these air-bearing amplitudes the typical damping uncertainty is about 30%.
- A resonance shift is not recognized going from the 1" to the 0.2" data cloud. This shows that a second time constant from contact angle hysteresis is absent.

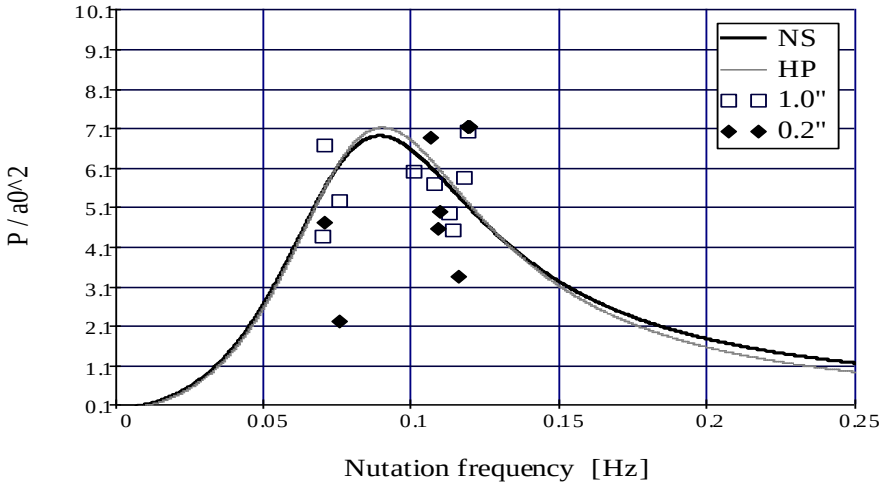

Fig-11 *NS model results and PTM experiments of the COS-B ND behavior at the extreme small flight nutation angle 1.0" and 0.2" in the vicinity of 0.105 Hz (=0.661 rad/s) with nominal flight liquid temperature T = 7.5 ^{0}C.*

5 Conclusions

The ND verification and validation data of the following three classes of S/C were investigated:

1. The 5 rpm Ulysses and 15 rpm Cluster S/C flight data mention nominal ND performance but these yield no explicit data or in-orbit invoked nutation experiments.
2. The meteorological 100 rpm MSG S/C yields in-orbit AOCS compliance with the ND design.
3. The EQUATOR-S at 48-50 rpm and COS-B S/C 9.45-17.63 rpm records yield very interesting data. A systematic model comparison was conducted yielding the following results:

The relative amount of COS-B liquid mass, with requirement $m/M << 1$ as prerequisite of a quasi-rigid S/C configuration, is about one third of the EQUATOR-S value. The "free liquid" k_0 factor accounting for the applicability of the RHP model is comparable.

The EQUATOR-S RHP (Refined Hagen-Poiseuille Model) flight damping time constant prediction is within 15% compared to the NS and HP model. Peculiar is the fact that the RHP model which drove the ND design, shows a -3% resonance offset from the design value $\lambda_o = 1.33$.

The EQUATOR-S ND design data given by [Häusler and Eidel, 2001] and [Häusler et al., 2002] do not reveal an essential picture with the modeled time constant as a function of the S/C inertia ratio λ. The frequency tuning of the ND is not mentioned but only the agreement in damping time constant between the RHP model results, air-bearing verification data and flight results at nominal flight conditions. The considerable -3% offset from the ND resonance frequency (with consequently optimum damping) indicates that the mass of the EQUATOR-S ND could have been reduced.

It can be concluded that the NS model derived in the co-rotating S/C body reference frame is the backbone of ND design on basis of its superior V&V status.

The plexi-glass PTM model of the EQUATOR-S ND has totally different end pot materials, surface treatment (if any) and RMS roughness compared to the Aluminum FM. Despite these differences the PTM tests show a good RHP based agreement with the FM flight and ground test damping time constant results.

The Dutch Space COS-B flight nutation data have been embedded in the HP, RHP and NS model predictions. At the spin-rates 9.45 and 17.63 rpm excellent damping performance agreement was found with the developed HP and NS MathCad® coded models. The RHP model shows an additional resonance off-set of 4% compared to the NS and HP modeling. In both cases, the RHP model and its time constant prediction is far off and does not comply with the COS-B design and its flight performance validation.

The COS-B ultimate damping angle tests with the PTM glass model did not reveal a second time constant due to end pot hysteresis phenomena. This is concluded after studying and re-analyzing the results of a high number of repetitive tests at 1.0 and 0.2" ultimate angles in air-bearing tests. An ultimate nutation angle analysis for the EQUATOR-S ND design is not given.

Literature

Agrawal B., *Dynamic Characteristics of Liquid Motion in Partially Filled Tanks of a Spinning Spacecraft*, AIAA Journal of Guidance, Control, and Dynamics, Vol. 16, No. 4, July-August, 1993, pp. 636-640.

Ancher L.J. , van den Brink H. and Pouw A., *Asymmetric oscillation of a passive nutation damper*, Fokker-VF The Netherlands. Study on passive nutation dampers performed under ESA contract 2318/74 Volume I, II and III (Appendices). Proc. of the CNES-ESA Conf. on 'Attitude Control of Space Vehicles – Technological and dynamical problems associated with the presence of Liquids' , ESA SP-129, pp. 179-183, 1977

Bakel C. van, *On the behaviour of the tube-with-endpots nutation damper* – UCN & Eindhoven University of Technology, WFE document 93.105 – August 1993.

Batchelor G.K. - An Introduction to Fluid Dynamics - Cambridge University Press, Chapter 4, 1980

Bongers E., 1984, In-orbit Experiments on COS-B nutation damper performance, ESA report TR-R-84-037

Boyd, D. and Kuiper, H., *The Compound Parabolic/elliptic Lightshades: Near-Optimal Shading for Cold Radiators*, SAE Technical Paper 2000-01-2278, 2000, doi:10.4271/2000-01-2278.

COS-B S/C mission description http://sci.esa.int/science-e/www/object/index.cfm?fobjectid=31447 and http://www.esa.int/esaSC/120375_index_0_m.html

COS-B S/C (2), ESA bulletin no2, special August 1975

Crowden J.B., Fax No92927190 from Marconi Space Systems / Aerospatiale Cannes, Nutation Dampers for 2nd generation Meteosat, 22-01-1990

Ebert K. and Reger G., SLOSHING ANALYSIS FOR METEOSAT SECOND GENERATION, Proc. 2nd European Spacecraft Propulsion Conference, ESA SP-398, August 1997.

Enderle W. and Feucht U., Attitude Control Simulation for EQUATOR-S Using Object Oriented Modeling, GSOC DLR Oberpfaffenhofen, Proc. 3rd Int. Conf. on spacecraft GNCS, ESTEC. ESA SP-381, 1997

Häusler B. and Eidel W., *Ein Flüssigkeitsnutationdämpfer für den Satellit EQUATOR-S* , Forschungsbericht: LRT-WE-9-FB-1, Institut für Luft und Raumfahrttechnik, Universität der Bundeswehr München, Neubiberg, Germany, 2001

Häusler B., Eidel W. and Stöcker J., *Ein Flüssigkeitsnutationdämpfer für den Satellit EQUATOR-S*, Forschung im Ingenieurwesen, 67, 27-39, 2002

Hong, J.Z., *Residual Nutation Angle of Satellites with Viscous Nutation Dampers*, Acta Astr. , Vol. 15, No. 1, pp. 1-7, 1987

Hughes Peter C., Spacecraft Attitude Dynamics, Chapter 4 - *Attitude Dynamics of a Rigid Body*, Chapter 5 - *Effect of Internal Energy Dissipation on the Directional Stability of spinning bodies*, John Wiley & S, 1986

Loitsyanskii L.G., *Mechanics of Liquids and Gases*, page 496 – 509, Pergamon Press, 1966

Luengo, O., *DYNAMIC MODEL OF THE MSG ATTITUDE, EUMETSAT* (GMV consultant), ESA Proceedings., ESASP.548-313L, 2004Muto T and Nakane K., *Unsteady flow in circular tube (velocity distribution of pulsating flow)*, Bulletin in the Japan society of Mechanical Engineering, 1980

Papanastasiou T.C., Georgiou G.C. and Alexandrou A.N., *Viscous Fluid Flow*, page 243-253, CRS Press 1999

Truckenbrodt E., *Strömungsmechanik* , Springer, Berlin Heidelberg, NY, 1996

Truckenbrodt A., Schultysik B. and Mehltretter J.P., *Nutationsdämpfer für den AMPTE-IRM Satelliten: Abschlußbericht*, Technology Consulting Institute for Applied Research GMBH (West Germany), TC-no. 017-Tru-SCh0/sa, 9 Dec. 1982

Weymiens B. , Oremus R., Battrick B. et al, *Meteosat Second Generation*, ESA Publications, ESA BR-153, ISBN 92-9092-634-1, 1999

Willmore A.P., *A PROPOSAL FOR AN X-RAY EXPERIMENT FOR COS-B*, Non-Solar X- and Gamma-Ray Astronomy, 50-53, IAU, 1970

Womersley J.R., *Method for the calculation of velocity, flow and viscous drag in arteries when the pressure gradient is known*, Journal of Physiology, **127**, 533–563, 1955.